values resulting from the approximate nature of the $^3\Pi_u$ potential and causing the computed lifetimes to be in error by about a factor of 2.

With reference to the problem of energetic molecular beam formation, the radiative lifetimes are sufficiently long that keV molecules can drift several meters without appreciable decay; the radiative lifetimes are relatively insensitive to external fields: Moderate fringe fields up to the order of 10^4 V/cm will not affect the decay. Whether or not those rotational levels which are susceptible to allowed predissociation can contribute effectively to molecular beam formation can only be judged when a more accurate estimate of the lifetime for this dissociation mode becomes available.

ACKNOWLEDGMENTS

We are indebted to Professor J. C. Browne and to Professor W. Lichten for discussion of the predissociation modes.

*Work performed under the auspices of the U.S. Atomic Energy Commission.

[1]W. Lichten, Phys. Rev. 120, 848 (1960); 126, 1020 (1962).

[2]G. H. Dieke, Phys. Rev. 47, 870 (1935); 60, 523 (1941).

[3]G. Herzberg, *Molecular Spectra and Molecular Structure*, 2nd ed. (Van Nostrand, Princeton, N.J., 1950), p. 416.

[4]Reference 3, p. 410.

[5]W. Lichten, Bull. Am. Phys. Soc. 7, 43 (1962).

[6]L. Y. C. Chiu, Phys. Rev. 40, 2276 (1964).

[7]C. Bottcher and J. C. Browne (private communication).

[8]J. R. Hiskes, Bull. Am. Phys. Soc. 13, 308 (1968).

[9]J. R. Hiskes, Phys. Rev. 180, 146 (1969).

[10]J. R. Hiskes, Nucl. Fusion 2, 38 (1962).

[11]J. C. Browne, J. Chem. Phys. 40, 43 (1964).

[12]C. B. Wakefield and E. R. Davidson, J. Chem. Phys. 43, 834 (1965).

[13]W. Kolos and L. Wolniewicz, J. Chem. Phys. 48, 3672 (1968).

[14]H. A. Bethe and E. E. Salpeter, *Quantum Mechanics of One and Two Electron Atoms* (Springer, Berlin, 1957), p. 250.

[15]See Ref. 3, p. 119. Our N is designated as J on p. 118 and as K in Chap. V of Ref. 3.

[16]B. L. Moisewitsch, Monthly Notices Roy. Astron. Soc. 117, 189 (1957).

[17]S. Huzinaga, Progr. Theoret. Phys. (Kyoto) 17, 162 (1957).

[18]A. S. Coolidge and H. E. James, J. Chem. Phys. 6, 730 (1938).

[19]A. Amemiya, Proc. Phys. Math. Soc. Japan 21, 394 (1939).

[20]G. H. Dieke, J. Mol. Spectry. 2, 494 (1958).

[21]H. Beutler and H. O. Jünger, Z. Physik 101, 285 (1936).

[22]W. M. Wright and E. R. Davidson, J. Chem. Phys. 43, 840 (1965).

[23]H. M. James and A. S. Coolidge, Phys. Rev. 55, 184 (1939).

PHYSICAL REVIEW A VOLUME 2, NUMBER 3 SEPTEMBER 1970

K-Shell Fluorescence Yields for Light Elements*

C. E. Dick and A. C. Lucas†

National Bureau of Standards, Washington, D.C. 20234

(Received 27 April 1970)

The K-shell fluorescence yield ω_K has been measured for the low-atomic-number elements beryllium, boron, carbon, fluorine, and magnesium. The primary vacancies in the K shell were produced by an intense beam of K x rays generated by electron bombardment of aluminum and carbon targets. The measured values of ω_K agree quite well with values calculated from a theoretical prediction of Wenzel. They exhibit only fair agreement with semiempirical formulas which include screening and relativistic effects, and with a recent calculation by McGuire based on the K-shell Auger transition rate.

I. INTRODUCTION

The occurrence of a vacancy in an atomic shell leads to an internal reorganization which ultimately results in the emission of a characteristic x ray or in the ejection of an Auger electron. Atomic excitation occurs in a wide range of processes, including nuclear decay by internal conversion and

electron capture and in the interaction of photons and charged particles with matter. If these phenomena are to be understood in detail, information on the atomic deexcitation process is essential.

The fluorescence yield ω_i for a particular atomic shell can be defined as the probability that an i-shell vacancy will result in the emission of a characteristic i-shell x ray. The Auger electron yield a_i can be defined in an analogous manner so that, in principle,

$$\omega_i + a_i = 1 . \tag{1}$$

In practice, caution must be exercised in the application of these definitions, since the existence of atomic subshells and the possibility of radiationless transitions between them can lead to confusion in the meaning of these constants. Only in the K shell can these definitions be applied in a straightforward manner, since deexcitation in this case can only occur through a fluorescent transition in which a K_α or a K_β x ray is emitted or through a radiationless transition in which an Auger electron is ejected.

The importance of these atomic constants has generated a large body of experimental data and theoretical calculations concerning their values. The most recent review of the subject of fluorescence-yield measurements has been given by Fink *et al.*[1] This tabulation of K-shell fluorescence yields, as well as earlier ones,[2,3] indicates that the measured values of ω_K for light elements show wide variations from one experiment to another and that values for elements lighter than magnesium are particularly scarce. The present experiment is designed to help fill this void by measuring ω_K for beryllium, boron, carbon, fluorine, and magnesium.

II. EXPERIMENTAL METHOD

In the present experiment, the K-shell vacancies were produced by an intense beam of K x rays generated by electron bombardment of aluminum or carbon targets.[4] The predominant mechanism by which photons having these energies (slightly greater than the K-shell binding energy of the fluorescer) interact in the fluorescer, is the photoelectric effect. Measurement of the number of fluorescence x rays produced leads to a determination of ω_K in a manner which is described below.

The experimental arrangement is shown in Fig. 1. A low-energy beam of electrons in the region from 20 to 40 keV was produced by the National Bureau of Standards (NBS) 0.5-MeV constant-potential accelerator and directed onto a target located in the center of an electrically isolated scattering chamber. The K x-ray beam generated

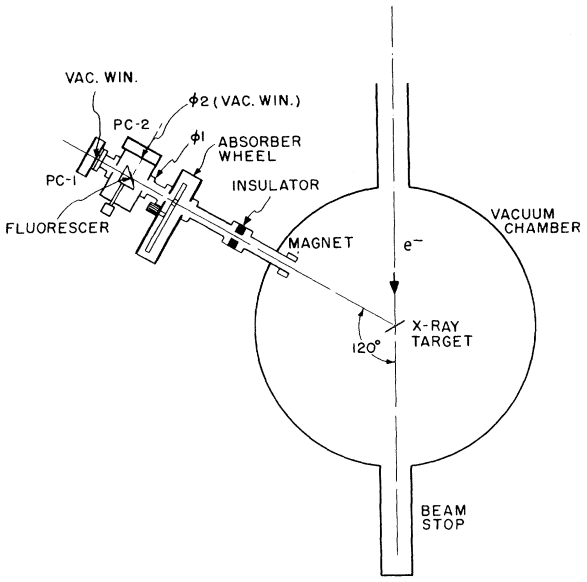

FIG. 1. Experimental arrangement for measuring the K-shell fluorescence yields.

in the target was collimated at a mean takeoff angle of 120° with respect to the incident electron direction by the aperture Φ_1, and allowed to impinge on the fluorescer inclined to the primary x-ray direction at an angle of 45°. K x rays produced in the fluorescer were detected at 90° with respect to the primary x-ray beam by a proportional counter PC-2 which subtends a solid angle ($\Omega_2 = 9.97 \times 10^{-3}$ sr) at the fluorescer defined by the aperture Φ_2. This aperture also supported the counter window. A second nearly identical proportional counter PC-1 was mounted on the axis of the primary x-ray beam so that *in situ* measurements of the primary x-ray flux can be made by withdrawing the fluorescer. An absorber wheel mounted in the beam line between the x-ray target and the fluorescer facilitated background- and proportional-counter-window transmission measurements. A small permanent magnet around the beam path inside the vacuum chamber prevented stray electrons from reaching the fluorescer.

The target geometry and the 120° scattering angle shown in Fig. 1 were chosen to enhance the purity and intensity of the primary x-ray beam.[4] The x-ray targets were fabricated from sheets of a aluminum and graphite. In addition, targets of beryllium, boron nitride (BN), teflon $[(-CF_2-)_n]$, and magnesium were used to generate the x-ray beams used to measure the attenuation in proportional counter windows for these characteristic photon energies as described below. In all cases the range[5] of the incident electrons was less than the

TABLE I. Typical proportional counter parameters.

Element	Counting gas	Pressure	Window material	Window transmission	Efficiency
Be	CH_4	3 cm	Collodion	0.25	0.724
B	$10\%A + 90\%CH_4$	3 cm	Collodion	0.50	0.996
C	$10\%A + 90\%CH_4$	3 cm	Collodion	0.75	0.915
F	$10\%A + 90\%CH_4$	3 cm	Collodion	0.65	0.536
Mg	$90\%A + 10\%CH_4$	1 atm	Polypropylene	0.85	0.999
Al	$90\%A + 10\%CH_4$	1 atm	Polypropylene	0.90	0.991

target thicknesses. X-ray–yield measurements were monitored by measuring the total charge incident on the target with a precision digital charge integrator to an accuracy of better than 1%.

The proportional counters PC-1 and PC-2 used to measure the primary and scattered x rays were operated in the flow mode with argon-methane gas mixtures. They were isolated from the fluorescer chamber by thin organic windows. The counters were fabricated in the form of a right circular cylinder 3.175 cm in diameter by 10-cm long with a 0.05-mm stainless-steel central wire operated at positive high voltage. The windows were mounted to allow radiation to enter the active volume at the midplane and perpendicular to the counter axis. The attenuation of each window was measured for each radiation of interest by placing it in the absorber wheel and inserting it into the x-ray beam. The corresponding efficiencies were calculated for the appropriate counting gas using values of the absorption coefficients tabulated by Henke *et al.*[6] Relative efficiency values were also verified by observing the counting rate as a function of gas pressure for the several mixtures used. Typical values for the counter parameters are listed in Table I.

Besides facilitating the measurement of window thickness, the absorber wheel allowed the insertion of various absorbing materials into the primary x-ray beam so that background corrections could be made. The effect on the primary beam of alternately inserting aluminum and magnesium Ross filters into an x-ray beam generated in an aluminum target is shown in Fig. 2. These spectra show that although the magnesium filter reduces the intensity in the K line by approximately two orders of magnitude, the spectrum outside of this region is nearly identical for the two filters. This pair of filters was used for all measurements employing an x-ray beam generated using an aluminum target. For the measurements employing a C x-ray beam, a carbon-boron Ross filter pair was not available, so a detailed examination of the effect of a thin, 0.3-mg/cm^2 polypropylene filter was made. The effect of this filter could be measured to a few percent, and fluorescence yields from materials excited by C x rays were measured both with and without this filter.

Pulse-height spectra from PC-2 were recorded for periods ranging from a few minutes to a few hours. Several separate determinations for each material and average data are reported. Typical fluorescence spectra for magnesium are shown in Fig. 3. The difference between the two spectra in Fig. 3 corresponds to the magnesium fluorescence generated by aluminum x rays (the difference between the two spectra in Fig. 2). Counts in PC-2 were determined to be totally attributable to

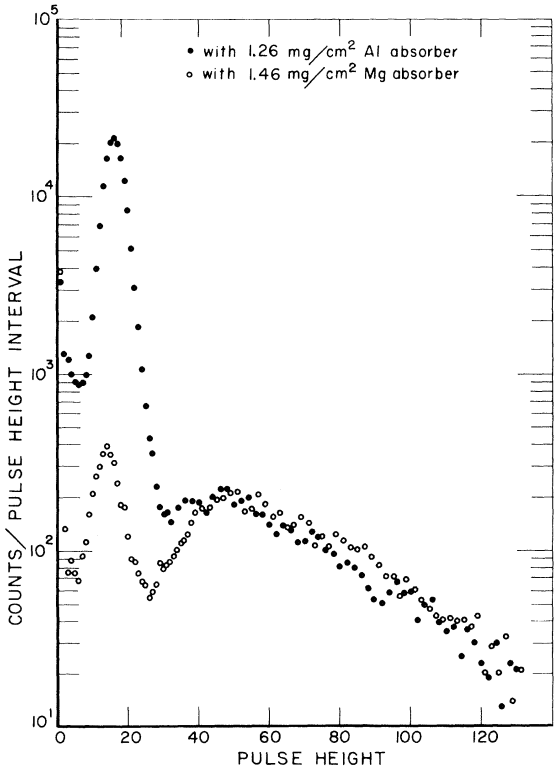

FIG. 2. Primary aluminum x-ray spectra recorded in proportional counter PC-1 in Fig. 1. The effects of filtering the primary beam with a Ross pair of aluminum and magnesium filters is shown.

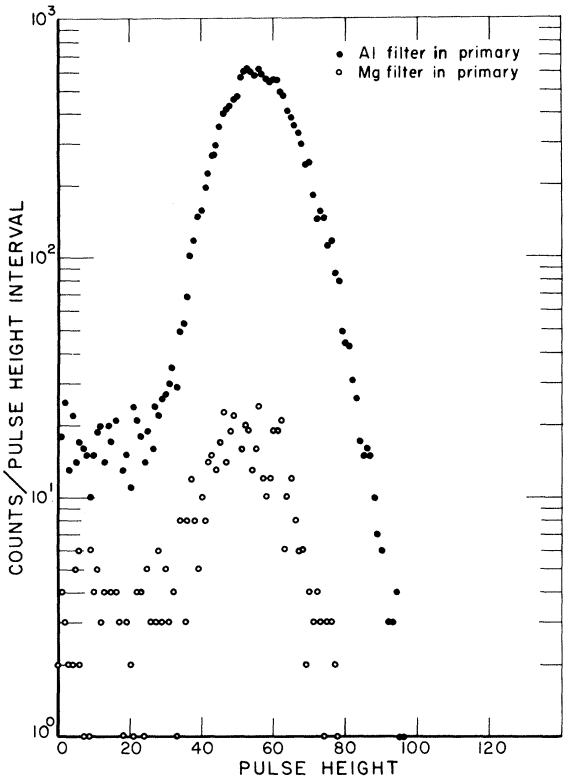

FIG. 3. Magnesium fluorescence x-ray spectra produced by the primary aluminum spectra shown in Fig. 2.

x rays generated in the fluorescer by retracting it from the beam, in which case the counting rate in PC-2 decreased to essentially zero.

In addition to K x rays generated in the fluorescer by the primary x-ray beam, K fluorescence may be excited by two other sources: (i) photons in the bremsstrahlung continuum from the x-ray target and (ii) secondary photoelectrons generated in the fluorescer. The first of these was accounted for by the use of the filtering technique described above. The possible contribution from the latter was investigated by measuring the K-fluorescence yield from beryllium and boron with both carbon and aluminum primary beams. This has the effect of varying the secondary photoelectron energy. No difference in the K-fluorescence yield was observed for either beryllium or boron under these conditions. This is in agreement with the results of Birks *et al.*,[7] who found that the cross section for the production of K x rays by electrons near threshold was orders-of-magnitude smaller than that for production by photons.

For the fluorescer geometry shown in Fig. 4, the number of scattered K x rays per st N_f produced in the target between x and $x+dx$ is given by

$$N_f = \int_0^t \frac{N_i}{4\pi} \exp[-x\mu_i/\cos\theta_1]\,\mu_i \times f\omega_K \exp[-x\mu_f/\cos\theta_2]\,\frac{dx}{\cos\theta_1}\,, \tag{2}$$

where N_i is the number of photons in the primary beam, μ_i is the absorption coefficient for the primary photons in the fluorescer, ω_K is the K-shell fluorescence yield, and μ_j is the absorption coefficient for self-absorption of the fluorescence radiation in the scatterer. The exponential terms account for the attenuation of the primary and fluorescence photons in passing in and out of the target. The number of K vacancies created is given by $\mu_i f$, where f is the fraction of all interactions which yield K vacancies. The quantity f is determined from the jump in the absorption of the target material at the K edge. Thus,

$$f = (\mu_H - \mu_L)/\mu_H = 1 - 1/r = (r-1)/r, \tag{3}$$

where r is the so-called absorption jump ratio at the K edge, and μ_H and μ_L are the absorption coefficients above and below the K edge, respectively.

In the present experiment, $\theta_1 = \theta_2 = 45°$. For a fluorescer of thickness much greater than the range of the primary photon, Eq. (2) may be integrated to give

$$N_f = (N_i f\omega_K/4\pi)[\mu_i/(\mu_i+\mu_f)]. \tag{4}$$

Since the fluorescence x rays are detected in a proportional counter having an efficiency ϵ for these photons, a window transmission τ, and subtending a solid angle of Ω_2 st at the fluorescer,

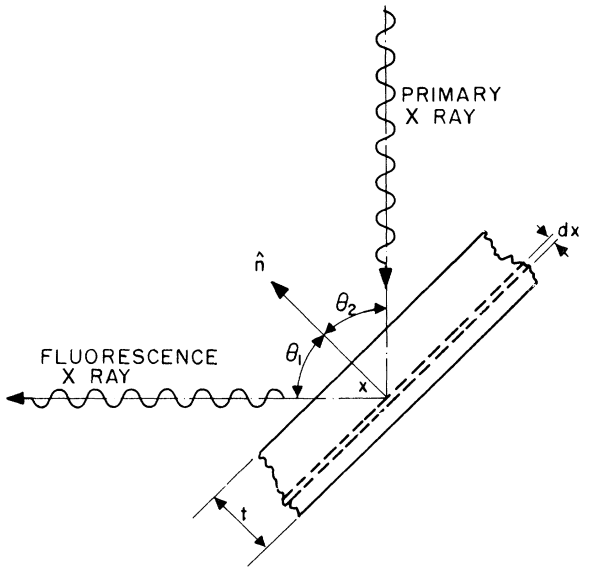

FIG. 4. Fluorescer geometry.

TABLE II. Typical experimental data and results for each fluorescer.

Element	Filter (Ross pair)	Primary energy (ev)	N_i (10^{10})	$g(A)$ [Eq. (7)]	N_2 (typical)	ω_K (typical)
Be	none	378(C)	4.81	1.0	1902	2.69×10^{-4}
B (in BC)	none	378(C)	2.22	0.7	4304	6.20×10^{-4}
C	none	1487(Al)	2.22	1.0	2363	1.22×10^{-3}
F (in CF_2)	Al-Mg	1487(Al)	1.11	0.76	3340	6.30×10^{-3}
Mg	Al-Mg	1487(Al)	0.22	1.0	14650	2.26×10^{-3}

Eq. (4) may be used to solve for N_2, the number of fluorescence x rays detected in PC-2. Thus,

$$N_2 = f\omega_K(\Omega_2\epsilon\tau/4\pi)[\mu_i/(\mu_i+\mu_f)] . \quad (5)$$

Combining Eqs. (5) and (3) and solving for ω_K, we get the desired result

$$\omega_K = \frac{4\pi}{\Omega_2}\frac{N_2}{N_i}\frac{1}{\epsilon\tau}\frac{r}{r-1}\left(\frac{\mu_i+\mu_f}{\mu_i}\right) . \quad (6)$$

This equation may be generalized in the case of a compound fluorescer containing two elements A and B to

$$\omega_{K(A)} = 4\pi N_{2(A)}/[\Omega_2 N_i \epsilon_{(A)}\tau_{(A)}][r_{(A)}/r_{(A)}-1] \times[g_{(A)}(\mu_i+\mu_A)+h_{(B)}(\mu_{iB}+\mu_{AB})/g_{(A)}\mu_{iA}], \quad (7)$$

where μ_{ik} is the absorption coefficient for photon l in intrinsic material k, and $g_{(A)}$ and $h_{(B)}$ give the fractional composition of elements A and B in the fluorescer material.

Equations (6) and (7) were used to calculate the value of ω_K from the side counter yields N_2. The values of the absorption coefficients and the absorption-edge jump ratios were taken from the tables of Henke.[6] The uncertainty in the fluorescence yields arising from uncertainties in these values was determined by evaluating Eqs. (6) and (7) for values of the absorption coefficients which were ±10% different from the tabulated values with a corresponding change in r calculated from Eq. (3).

III. RESULTS

Three or more runs on each fluorescer were made using the C or Al x rays which could excite fluorescence. Typical data for each element are given in Table II.

The uncertainties in the quantities used to evaluate ω_K from Eqs. (6) or (7) are listed in Table III. The resulting uncertainty in ω_K was taken to be $2(\sum\Delta_i^2)^{1/2}$, where Δ_i is the uncertainty in ith one of these quantities. This assignment was made to include possible systematic errors which are impossible to determine by simple repetition of the experiment. For this reason, the uncertainty assigned to ω_K was that taken for a single measurement, although the repeatability of the measurements in all cases was better than ±15%. The measured values of ω_K as a function of Z are given in Fig. 5. The error bars shown are those calculated from Table III. Also included in Fig. 5 are other experimental values[8–17] for elements from beryllium to aluminum. These values and the present experimental results are listed in Table IV. It should be pointed out that the uncertainties quoted in Table III for the side-counter yield N_2 include those arising from background corrections from bremsstrahlung and possible secondary photoelectric contamination and are not purely due to counting statistics. The large uncertainties in the window transmission for the boron measurements are due to the fact that the boron x rays used to measure the window thickness were generated in a BN target, and complete separation of the B and N x rays was difficult.

IV. DISCUSSION

The problem of calculating theoretical values

TABLE III. Uncertainties in the quantities used to evaluate ω_K by Eqs. (6) or (7).

Element	Incident flux N_i	Window transmission τ	Counter efficiency ϵ	$\frac{r}{r-1}$	$\left\{\frac{\mu_i+\mu_f}{\mu_i}\right\}$[a]	N_2	Geometrical factors ($\Omega_2, \theta_1, \theta_2$, etc.)
Be	±5%	±5%	±5%	±1%	±2%	±5%	±1%
B	±5%	±10%	±5%	±1%	±4%	±5%	±1%
C	±5%	±5%	±5%	±1%	±8%	±3%	±1%
F	±5%	±5%	±5%	±2%	±4%	±2%	±1%
Mg	±5%	±5%	±3%	±2%	±1%	±1%	±1%

[a] In the case of compound targets the appropriate expression from Eq. (7).

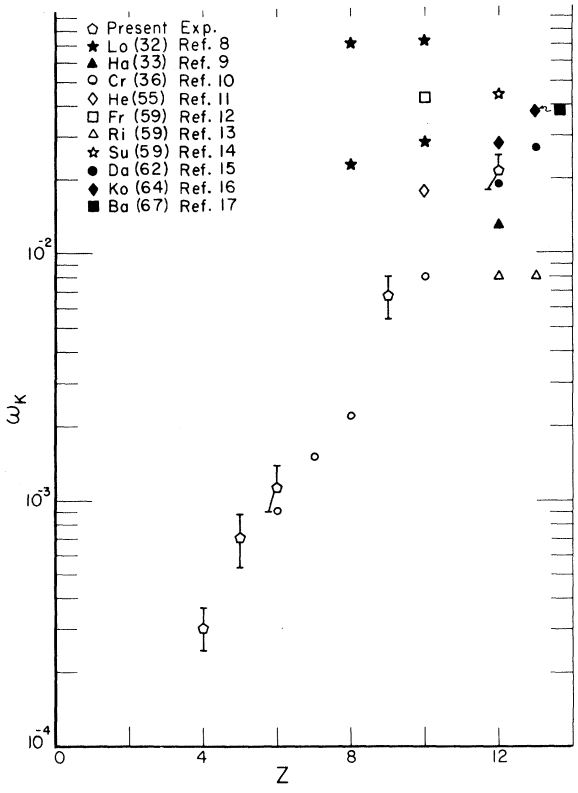

FIG. 5. Experimentally measured values of the K-shell fluorescence yield ω_K for elements between beryllium and aluminum.

for ω_K has been studied by a large number of investigators.

Wentzel[18] estimated that the Auger electron yield α_K should be independent of Z while ω_K should vary roughly as Z^4, since the K_α and K_β transitions are of the electric-dipole type and expressed $\omega_K(Z)$ in the form

$$\omega_K(Z) = (1 + A/Z^4)^{-1}, \tag{8}$$

with $A \approx 10^6$. This estimate included only the L-shell participation in the Auger process and ignored screening and relativistic effects. Burhop[19] has pointed out that transitions involving the M and N shells may be taken into account if the following values of A are used in Eq. (8): $A = 9\times10^5$ for $Z < 10$; $A = 1.19\times10^6$ for $10 \leq Z \leq 18$; and $A = 1.27\times10^6$ for $Z > 18$.

Burhop[20] has also derived the following semiempirical formula:

$$\omega_K/(1-\omega_K) = [A + BZ + CZ^3]^4, \tag{9}$$

where the constants A and C account for screening and relativistic effects, respectively. Various fits have been made to this expression, the latest being those of Hagedoorn and Wapstra[21] who found the following values of the constants: $A = -6.4\times10^{-2}$; $B = 3.15\times10^{-2}$; and $C = 1.03\times10^{-6}$; and of Bailey and Swedlund[17] who fitted Eq. (9) with the values $A = 4.08\times10^{-2}$; $B = 3.15\times10^{-2}$; and $C = -8.28\times10^{-7}$ for $Z \geq 13$. It should be noted that the primary difference between these two calculations is the difference in sign for the screening parameter A.

These theoretical estimates are all derived assuming that the Auger transition rate is independent of Z. Bailey and Swedlund[17] point out, however, that an examination of the radiation transition widths used in an Auger transition-rate calculation by Callen[22] indicate that these transition rates are directly proportional to Z. This negates the assumption used in the postulation of Eq. (9) and, in fact, leads to a new formula

$$\omega_K/(1-\omega_K) = (A + BZ + CZ^3)^3, \tag{10}$$

where the *cubic* replaces the *quartic* power. Bailey and Swedlund[17] fitted their data to this formula and derived the following values: $A = -0.1019$; $B = 3.377\times10^{-2}$; and $C = -1.177\times10^{-6}$, where the sign of the screening term is negative and the relativistic correction now has the positive sign. We have not fitted our data to any of the above formulas owing to the limited range of elements for which we took data. We have, however, compared our results with Eqs. (8)–

TABLE IV. Experimental values of ω_K for elements from beryllium to aluminum.

Z	Element	ω_K	Reference
4	Be	$(3.04\pm0.61)\times10^{-4}$	Present work
5	B	$(7.10\pm1.84)\times10^{-4}$	Present work
6	C	$(1.13\pm0.24)\times10^{-3}$	Present work
		$(0.9\ \pm\cdots)\times10^{-3}$	Crone (1936)[a]
7	N	$(1.5\ \pm\cdots)\times10^{-3}$	Crone (1936)[a]
8	O	$(8.2\ \pm\cdots)\times10^{-2}$	Locher (1932)[b]
		$(2.3\ \pm\cdots)\times10^{-2}$	Locher (1932)[b]
		$(2.2\ \pm\cdots)\times10^{-2}$	Crone (1936)[a]
9	F	$(6.7\ \pm1.34)\times10^{-3}$	Present work
10	Ne	$(8.3\ \pm\cdots)\times10^{-2}$	Locher (1932)[b]
		$(4.3\ \pm0.4\ )\times10^{-2}$	Frey *et al.* (1959)
		$(2.8\ \pm\cdots)\times10^{-2}$	Locher (1932)[b]
		$(1.8\ \pm0.4\ )\times10^{-2}$	Heintze (1955)
		$(8.1\ \pm0.4\ )\times10^{-2}$	Crone (1936)
11	Na		
12	Mg	$(4.5\ \pm0.2\ )\times10^{-2}$	Suzor and Charpak (1959)
		$(2.8\ \pm0.11)\times10^{-2}$	Konstantinov *et al.* (1964)
		$(2.15\pm0.36)\times10^{-2}$	Present work
		$(1.9\ \pm\cdots)\times10^{-2}$	Davidson and Wyckoff (1962)
		$(1.3\ \pm0.3\ )\times10^{-2}$	Haas (1933)
		$(0.8\ \pm0.3\ )\times10^{-3}$	Rightmire *et al.* (1959)
13	Al	$(3.81\pm0.15)\times10^{-2}$	Konstantinov (1964)
		$(3.79\pm0.23)\times10^{-2}$	Bailey and Swedlund (1967)
		$(2.7\ \pm\cdots)\times10^{-2}$	Davidson and Wyckoff (1962)
		$(0.8\ \pm0.3\ )\times10^{-2}$	Rightmire *et al.* (1959)

[a]Relative to a value of $\omega_K(\mathrm{Ne}) = 8.1\times10^{-3}$.

[b]Two values for each element measured by Locher arise from the use of two different sets of μ/ρ values.

TABLE V. Comparison of the experimental and calculated values of ω_K.

Element	Experiment	Eq. (8) with A taken for $M \pm N$ shell (Ref. 20)	Eq. (9) Fourth power law Constants from (Ref. 21)	Eq. (9) Fourth power law Constants from (Ref. 17)	Eq. (10) third-power law (Ref. 17)	McGuire (Ref. 23)
Be	$(3.04 \pm 0.61) \times 10^{-4}$	2.8×10^{-4}	2.7×10^{-5}	7.72×10^{-4}	3.63×10^{-5}	...
B	$(7.10 \pm 1.84) \times 10^{-4}$	6.9×10^{-4}	1.25×10^{-4}	1.54×10^{-3}	2.98×10^{-4}	8.5×10^{-4}
C	$(1.13 \pm 0.24) \times 10^{-3}$	1.44×10^{-3}	3.81×10^{-4}	2.77×10^{-3}	1.01×10^{-3}	3.5×10^{-4}
F	$(6.70 \pm 1.34) \times 10^{-3}$	7.24×10^{-3}	3.37×10^{-3}	1.08×10^{-2}	8.30×10^{-3}	1.4×10^{-2}
Mg	$(2.15 \pm 0.36) \times 10^{-2}$	1.71×10^{-2}	1.35×10^{-3}	2.95×10^{-2}	2.66×10^{-3}	3.4×10^{-3}

(10), and the results are shown in Table V.

Recently, McGuire[23] has calculated the K-shell Auger transition rates and the fluorescence yields for the elements from boron through argon. These values are also given in Table V. Comparison of our results with this calculation indicates that the experimental values are consistently lower than these values. McGuire[23] points out that his values are about 25% higher than the measured values[16,17] for aluminum.

Recently, Byrne and Howorth[24] have fit the experimental data to an eighth-order polynomial, but comparison with their expression is not possible, since they did not tabulate the numerical results of this comparison.

Examination of Table V indicates that our data are in good agreement with the simple expression Eq. (8) and give fair agreement with the third-power law, Eq. (10), for carbon, fluorine and magnesium. The wide ranges of values encountered in evaluating Eq. (9) for the two different sets of parameters indicate the importance of the screening parameter A for low Z where the relativistic corrections are essentially unimportant. The third-power calculation with negative screening underestimates the measured value of ω_K for Be and B which indicates that for these elements screening is negligible, as might be expected.

ACKNOWLEDGMENT

The authors would like to acknowledge the assistance of Jeffrey R. Fuhr, Dr. R. C. Placious, and Julian H. Sparrow in the design and construction of the experimental apparatus.

*Work supported by the Defense Atomic Support Agency.

†Present address: EG&G, Incorporated, Goleta, Calif.

[1]R. W. Fink, R. C. Jopson, H. Mark, and C. D. Swift, Rev. Mod. Phys. 38, 513 (1966).

[2]C. Broyles, D. Thomas, and S. Haynes, Phys. Rev. 89, 715 (1953).

[3]M. A. Listengarten, Izv. Akad. Nauk SSSR, Ser. Fiz. 24, 1041 (1960) [Bull. Acad. Sci. USSR, Phys. Ser. 24, 1050 (1960)].

[4]The feasibility of producing such beams was suggested by detailed investigations on K x-ray production by J. W. Motz, C. E. Dick, A. C. Lucas, R. C. Placious, and J. H. Sparrow, Natl. Bur. Std. (unpublished).

[5]M. J. Berger and S. M. Seltzer, *Tables of Energy Losses and Ranges of Electrons and Positrons* (Office of Technical Services, Department of Commerce, Washington, D.C., 1964).

[6]B. L. Henke, R. L. Elgin, R. E. Lent, and R. B. Ledingham, Norelco Reptr. 14, 112 (1967).

[7]L. S. Birks, R. E. Seebold, A. P. Batt, and J. S. Grosso, J. Appl. Phys. 35, 2578 (1964).

[8]G. L. Locher, Phys. Rev. 40, 484 (1932).

[9]M. Haas, Ann. Physik 16, 473 (1933).

[10]W. Crone, Ann. Physik 27, 405 (1936).

[11]J. Heintze, Z. Physik 143, 153 (1955).

[12]W. F. Frey, R. E. Johnston, and J. I. Hopkins, Phys. Rev. 113, 1057 (1959).

[13]R. A. Rightmire, J. R. Sumanton, and T. P. Kohman, Phys. Rev. 113, 1069 (1959).

[14]F. Suzar and G. Charpak, J. Phys. Radium 20, 462 (1959).

[15]F. D. Davidson and R. W. G. Wyckoff, J. Appl. Phys. 33, 3528 (1962).

[16]A. A. Konstantinov, V. V. Perepelkin, and T. E. Sazonova, Izv. Akad. Nauk. SSSR, Ser. Fiz. 28, 107 (1964) [Bull. Acad. Sci. USSR, Phys. Ser. 28, 103 (1964)].

[17]L. E. Bailey and J. B. Swedlund, Phys. Rev. 158, 6 (1967).

[18]G. Wentzel, Z. Physik 43, 524 (1927).

[19]E. H. S. Burhop, in *The Auger Effect and Other Radiationless Transitions* (Cambridge U. P., Cambridge, England, 1952).

[20]E. H. S. Burhop, J. Phys. Radium 16, 625 (1955).

[21]H. L. Hagedoorn and A. H. Wapstra, Nucl. Phys. 15, 146 (1960).

[22]E. J. Callan, Proceedings of the International Conference on the Role of Atomic Electrons in Nuclear Transformations, 1963, p. 419 (unpublished).

[23]E. J. McGuire, Phys. Rev. 185, 1 (1969).

[24]J. Byrne and N. Howorth, J. Phys. B 3, 280 (1970).